International Journal of Pharmaceutics 642 (2023) 123101

Contents lists available at ScienceDirect

International Journal of Pharmaceutics

journal homepage: www.elsevier.com/locate/ijpharm

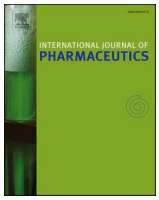

3D screen printing technology enables fabrication of oral drug dosage forms with freely tailorable release profiles

Marcel Enke [a], Nicolle Schwarz [a], Franka Gruschwitz [a], Daniela Winkler [a], Felix Hanf [a], Lisa Jescheck [a], Stefan Seyferth [b], Dagmar Fischer [b,c], Achim Schneeberger [a,*]

[a] Laxxon Medical GmbH, Hans-Knöll-Str. 6, 07745 Jena, Germany
[b] Division of Pharmaceutical Technology and Biopharmacy, Department of Chemistry and Pharmacy, Friedrich-Alexander-Universität Erlangen-Nürnberg (FAU), Cauerstr. 4, 91058 Erlangen, Germany
[c] FAU NeW, Nikolaus-Fiebiger-Strasse 10, 91058 Erlangen, Germany

ARTICLE INFO

Keywords:
3D printing
Additive manufacturing
Controlled release
Immediate-release
Extended-release
Paracetamol
3D screen printing
Drug delivery system

ABSTRACT

3D printing offers new opportunities to customize oral dosage forms of pharmaceuticals for different patient populations, improving patient safety, care, and compliance. Although several notable 3D print technologies have been developed, such as inkjet printing, powder-based printing, selective laser sintering (SLS) printing, and fused deposition modelling (FDM), among others, their capacity is often limited by the number of printing heads. 3D screen-printing (3DSP) is based on a classic flatbed screen printing that is widely used in industrial applications for technical applications. 3DSP can build up thousands of units per screen simultaneously, enabling mass customization of pharmaceuticals. Here, we use 3DSP to investigate two novel paste formulations: immediate-release (IR) and extended-release (ER) using Paracetamol (acetaminophen) as the active pharmaceutical ingredient (API). Both disk-shaped and donut-shaped tablets were fabricated using one or both pastes to design drug delivery systems (DDS) with tailored API release profiles. The size and mass of the produced tablets demonstrated high uniformity. Characterization of the tablets physical properties, such as breaking force (25–39 N) and friability (0.002–0.237%), adhering to Ph. Eur (10th edition). Finally, drug release tests with a phosphate buffer at pH 5.8 showed Paracetamol release depended on the IR- and ER paste materials and their respective compartment size of the composite DDS, which can be readily varied using 3DSP. This work further demonstrates the potential of 3DSP to manufacture complex oral dosage forms exhibiting custom release functionalities for mass production.

1. Introduction

Three-dimensional printing (3DP) is an emerging manufacturing technology that is quickly gaining acceptance in the pharmaceutical industry (Elbadawi et al., 2021; Jamróz et al., 2018). Its ability to overcome the limitations of traditional production, such as enabling personalized pharmacotherapy and mass customization, have shown that it can be a useful tool to address dosing and treatment gaps among patients (Beg et al., 2020; Khairuzzaman, 2018; Seoane-Viaño et al., 2021; Tracy et al., 2023; Trenfield et al., 2019).

3DP offers a wide range of opportunities to smartly modify oral dosage forms in terms of size, shape, release profile, and dose modification at scale. Developed initially for industrial applications, numerous 3DP technologies have already shown promise for pharmaceutical development (Melnyk and Oyewumi, 2021), most notably: inkjet printing (Cader et al., 2019; Kyobula et al., 2017), powder-based printing (Infanger et al., 2019; Wang et al., 2006; Yu et al., 2007), selective laser sintering (SLS) printing (Awad et al., 2019), as well as key extrusion-based printing technologies like fused deposition modelling (FDM) (Goyanes et al., 2015a; Khaled et al., 2014; Pietrzak et al., 2015),

Abbreviations: API, active pharmaceutical ingredient; D, diameter; DDS, drug delivery system; 3DP, 3-dimensional printing; 3DSP, 3-dimensional screen printing; ER, extended release; FDA, Food and Drug Administration; H, height; HPC, hydroxypropyl cellulose; HPLC, High performance liquid chromatography; IR, immediate release; L, length; Rpm, rotations per minute; MCC, microcrystalline cellulose; SA, surface area; USP, United States Pharmacopeia; UV, ultraviolet; V, volume; W, width; Wt%, weight.

* Corresponding author.
E-mail address: achim.schneeberger@laxxonmedical.com (A. Schneeberger).

https://doi.org/10.1016/j.ijpharm.2023.123101
Received 18 April 2023; Received in revised form 29 May 2023; Accepted 30 May 2023
Available online 7 June 2023

and 3D screen printing (3DSP) (Enke et al., 2022; Moldenhauer et al., 2021). Although all of these technologies are variations of additive manufacturing, each 3DP technology uses a unique method to deposit material layers and to cure them (Awad et al., 2020, 2018; Firth et al., 2018; Robles Martinez et al., 2018; Trenfield et al., 2018). These technologies have varying potential to scale, from small-scale personalized medicine approaches up to mass market production capacity.

Despite increased appeal, widespread implementation of the 3DP technology for pharmaceuticals remains hindered by low mechanical resistance of tablets, low printing resolution, limited material choices, and a lack of appropriate regulatory frameworks (El Aita et al., 2019; Varghese et al., 2022). There are currently only a few 3D printed medicines that are FDA approved and marketed. These include the fast-release oral antiepileptic Spritam®, from Aprecia Pharmaceuticals (USA) created using Binder Jetting/Drop on Powder technology (West and Bradbury, 2018). Furthermore, Triastek have 3 different drugs (T19, T20, T21) in development with IND approval produced with the company's patented Melt-Extrusion Deposition (MED) technology, that continuously converts powder feedstocks into softened/molten states followed by precise layer-by-layer deposition (Triastek, Inc., 2022).

3DP technologies have the potential to greatly improve the oral route for drug administration, which remains the preferred route by the majority of consumers worldwide (Infanger et al., 2019; Wang et al., 2006; Yu et al., 2007). The global oral drug delivery market is forecasted to grow substantially in coming years, from USD 98.3 billion in 2020 to USD 148.2 billion in 2027 as the prevalence of chronic diseases accelerates (Research and Markets, 2022). The ability to precisely dose drugs to different patient populations, especially for drugs with a narrow therapeutic window, or for those drugs where side effects from both over- and underdosing are common, would allow for improved treatment regimens for these conditions, as well as a reduction in drug expenditure costs (Jose and Gv, 2018; Norman et al., 2017; Peck, 2021; Zhu et al., 2020).

However, the ability to provide a reliable and consistent product for the mass market relies on the control of the resolution and reproducibility of the printed layers. This will vary based on the paste rheology, speed of nozzle movement, nozzle thickness and the printing technology used. Inconsistent layer thickness and print patterns, insufficient adhesion between consecutive layers, and overly fragile tablets, can dramatically hinder commercialization potential (Mirza and Iqbal, 2019; Norman et al., 2017; Zhu et al., 2020). Although some of these issues arise from the technology used, most arise from the material properties of the formulation.

Previously, we have shown that 3DSP can be used to create a range of different sizes and geometries for oral dose tablets with an extended-release paste containing the drug Paracetamol (acetaminophen), highlighting the potential of 3DSP to fabricate more complex oral dosage forms for mass production with high reproducibility (Moldenhauer et al., 2021). 3DSP is a special type of extrusion printing that uses a screen mesh to transfer printing pastes onto a substrate. This approach is based on a classic flatbed screen printing that is widely used in industrial applications (Jurisch et al., 2015; Kipphan, 2001). Compared to other 3DP technologies, whose capacity is limited by the number of printing heads (Alhnan et al., 2016; Hsiao et al., 2018), 3DSP is not limited by the number of printing heads and can build up a much greater number of tablets simultaneously compared to other technologies, enabling the mass customization of pharmaceuticals. The technology is capable of printing small batches for R&D, up to commercial-scale production and has been successfully tested for tablets ranging from 5 mm to 20 mm.

Here we investigate the feasibility of manufacturing composite drug delivery systems with tailored drug release profiles using 3DSP technology based on pastes exhibiting different release profiles, in particular extended-release (ER) and immediate release (IR) formulations. To this end, pastes have been used alone or in combination to create 2-compartment drug delivery system (DDS) with tailored API release profiles. We report on the manufacturing of water-based pastes for 3DSP and measure the rheology of these pastes. Pastes were utilized to print ten different tablet types and their dissolution profiles were measured.

2. Materials and methods

2.1. Chemicals

Paracetamol (acetaminophen) was obtained from Caelo (Hilden, Germany). Avicel PH-105 was purchased from Dupont and glycerol and Triactin from AppliChem (Darmstadt, Germany). Calcium sulfate was supplied from Honeywell and talcum from Carlo ERBA. Silfar 350 was obtained from Wacker Chemie. Hydroxypropyl cellulose (Klucel EF and JXF), and Polyplasdone XL 10 was kindly provided by Ashland (Covington, KY, USA) and Starch 1500 by Colorcon (Dartford, UK). Pharmatose 350 M was kindly provided by DFE Parma. The blue dispersible color (TopMill® blue 260.36) was kindly supplied by Biogrund. Milli-Q water (18.2 MΩ cm) was used for all formulations and solutions. For HPLC-measurements, HPLC-grade solvents from Chemsolute (water and methanol) were applied.

2.2. Preparation of printing pastes

All pastes were mixed with a vacuum dissolver planetary mixer HRV-S 2DP from Herbst Maschinenfabrik GmbH (Buxtehude, Germany) with 3 agitator tools in a 2-liter glass container.

The immediate-release paste was formulated according to the composition in Table 1 at room temperature. A 10 wt% aqueous gel of Klucel EF Pharma was prepared. The appropriate amount of this binder gel (Table 1, Klucel EF Pharma) was then added into the 2-liter glass container of the planetary mixer. In the next step, all other ingredients were added into the glass container. The final paste was mixed for 20 min at 2500 rpm under 70 mbar vacuum.

The extended-release paste was formulated according to the composition in Table 2 under room temperature conditions. Klucel JXF Pharma with the necessary amount of water was processed to yield a 10 wt% gel solution. Subsequently, the prepared gel was transferred into the 2-liter glass container of the planetary mixer. All remaining ingredients were added into the glass container. The extended-release paste was mixed for 20 min at 2500 rpm under 70 mbar vacuum.

2.3. Rheology measurements

Rheology measurements were performed on a Kinexus Rheometer (Netzsch), equipped with a plate-plate geometry and a passive solvent trap. A 500 μm gap was selected. Measurements were performed at 25 °C. In the 3-Step-Shear rate test, shear rates of 0.1 s^{-1} (for 1.5 min), 100 s^{-1} (for 0.5 min) and 0.1 s^{-1} (for 6 min), were performed.

The approximate shear rates (Schröder, 2018) in the flooding process

Table 1
Composition of the immediate-release paste.

Component	Chemical name	Function	Wt%
Paracetamol	N-(4-Hydroxyphenyl)-acetamid	API	33.8
Klucel EF Pharma	Hydroxypropylcellulose	Binder	2.5
Polyplasdone XL 10	Crospovidone	Disintegrant	3.7
Avicel PH-105	Microcrystalline cellulose	Filler	3.0
Pharmatose 350 M	Lactose	Filler	5.3
Calcium sulfate	Calcium sulfate	Filler, Absorber	4.2
Glycerol	Propane-1,2,3-triol	Humectant	3.0
Talc	Magnesium silicate	Anti-tacking agent	0.3
Silfar 350	Polydimethylsiloxane	Anti-foaming agent	0.3
MilliQ Water	Water	solvent	43.9
Total			*100.0*

Table 2
Composition of the extended-release paste.

Component	Chemical name	Function	Wt%
Paracetamol	N-(4-Hydroxyphenyl)-acetamid	API	20.6
Klucel JXF Pharma	Hydroxypropylcellulose	Binder	5.8
Avicel P-105	Microcrystalline cellulose	Filler	2.7
Triacetin	Propane-1,2,3-triyl triacetate	Plasticizer	1.4
Glycerol	Propane-1,2,3-triol	Humectant	1.9
Talc	Magnesium silicate	Anti-tacking agent	1.6
Silfar 350	Polydimethylsiloxane	Anti-foaming agent	0.3
TopMill® blue 260.36	Dye based on indigo	Blue dispersible color	0.1
MilliQ Water	Water	Solvent	65.6
Total			*100.0*

were calculated by:

$$\dot{\gamma} = \frac{\nu}{h}$$

where ν stands for the speed of squeegee, and h stands for the wet film thickness.

For the printing process, the shear rates can be calculated as the shear rates in slot die extrusion using:

$$\dot{\gamma}_{app} = \frac{6Q}{bh^2}$$

with Q stands for the color application (volume flow of paste through the mesh while printing), and b and h stand for slit width and slit height, respectively.

2.4. 3D screen printing of tablets

Tablets were fabricated on a prototype lab production unit XHS STS 3D from Exentis Group AG as depicted in Fig. S1. The lateral tablet dimensions are determined by the used screen layouts (for example, see Fig. 1). Machine preparation for the printing process included mounting and alignment of the screen (manufactured by Buschkamp GmbH) and the squeegees, as well as the software set-up. Printer settings used were as follows: flooding and printing squeegee speed 100 mm s^{-1}, off-contact distance 2 mm, height increment for screen elevation 15 μm, dryer power 65% and drying time per layer 15 s (infrared-dryer). Tablets were printed on tempered glass plates (300 × 300 × 5 mm) with satin-finished surface. After printing was completed, the tablet-holding glass plates were further air-dried at room temperature overnight before the tablets could be easily removed with a razor blade. The lab printer can be equipped with one glass plate. The entire process to print and dry one tablet batch (one batch corresponds to 169 tablets) with the one paste takes approximately 1 to 1.5 h. To print tablets build of 2 pastes, the entire process needs 2 to 2.5 h due to addition cleaning steps of the screen and squeegees. Characterization of tablet morphology and mass uniformity was performed as previously described (Moldenhauer et al., 2021).

Ten different types of tablets were printed in total, of which 5 were disk-shaped tablets (9 mm × 2 mm, d × h) and 5 were donut-shaped tablets (10 mm × 4 mm × 2 mm, d_o × d_i × h). For each form, the following compositions were chosen IR only, ER only and IR to ER ratios of 1:1, 1:3 and 3:1.

2.5. Tablet hardness and friability testing

Resistance to crushing of tablets was determined according to the Ph. Eur. 2.9.8 (10th edition). Five tablets of each size and shape were tested with a Pharmatest PTB 511E. Data are reported as average ± standard deviation. Friability was tested as described in Ph. Eur. 2.9.7 (10th edition) with a change of the mass from 6.5 g to 2.5 g. Approximately 2.5 g tablets of each size and shape were dedusted with compressed air and weighed. Tablets were placed in the friability tester Pharmatest PTF 100 and rotated 100 times at a constant speed of 25 rpm. Following testing, the tablets were removed, dedusted and weighed. The friability as weight loss in % was calculated.

2.6. Mass uniformity

The weight variation test is carried out to ensure uniformity in the weight of tablets. The individual weight of 20 tablets from each formulation is determined and the average/variation is calculated to estimate mass uniformity.

2.7. Dimension uniformity

The dimension variation test is carried out to ensure uniformity in the dimension of tablets. 20 tablets from each formulation were measured with a Digimatic Caliper CD-15APX (certificated) and the average/variation is calculated to estimate dimension uniformity.

2.8. Disintegration testing

Disintegration was tested according to Ph. Eur. 2.9.1(10th Edition). Six tablets of each size and shape were tested with a Pharmatest Auto1EZ, an automatic disintegration time tester using discs. As test medium demineralized water (750 mL, 37 °C) was used. Data are reported as average ± standard deviation.

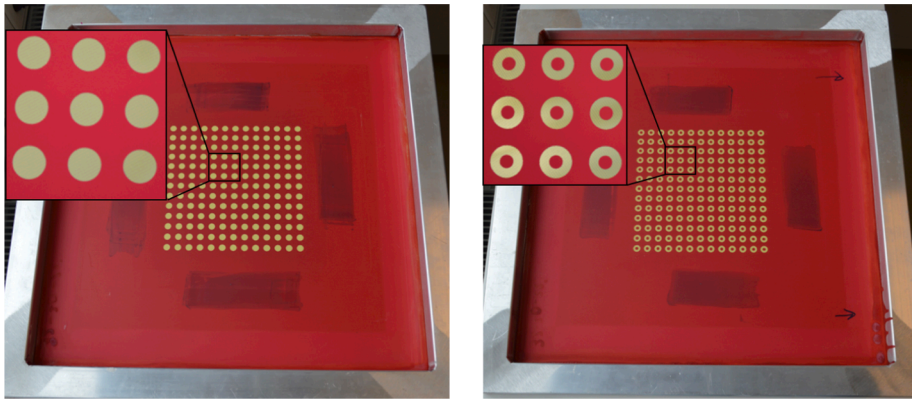

Fig. 1. Screen layout for disk-shaped tablet geometries (left) and donut-shaped tablet geometries (right). The magnifying inlets reveal the tablet geometries and the mesh in more detail. The screen size is 584 × 584 mm with a printing area of 180 × 180 mm, which can accommodate the printing of 169 tablets simultaneously. Disk-shaped tablets have a diameter of 9.165 mm. Donut-shaped tablets have an outer diameter of 10 mm and an inner diameter of 4 mm.

2.9. In vitro dissolution testing

Dissolution experiments were performed according to the USP monograph "Acetaminophen tablets" section dissolution of the US Pharmacopeia. A Vankel® VK 7000 dissolution paddle apparatus equipped with a VK750D heater were used for the dissolution experiments. Dissolution was performed using 900 mL phosphate buffer, pH = 5.8 at 37.0 ± 0.5 °C, with stirring at 50 rpm. Sink conditions were used. Wire claps were used to fix the tablets at the bottom of the vessel during the experiment.

Analysis (n = 6) was performed using a Thermo® Evolution 300 UV/Vis spectrophotometer equipped with flow-through cuvettes run by an Ismatec® IPS multichannel peristaltic pump. Absorption at λ = 243 nm was measured continuously over 8 h using the Thermo vision Pro software. A calibration curve in the range of 0.0147 – 1.1 mmol/l Paracetamol was made, which correlated with R = 0.9999.

3. Results and discussion

3.1. Printing tablets of different geometry and size

3D screen printing is a special form of additive manufacturing technology which utilizes a screen-mesh to simultaneously print a defined number of tablets layer-by layer, allowing for improved scalability and enabling mass production/customization of drug delivery systems compared to other available 3D printing technologies. 3D screen printing is based on the transfer of the API-containing printing paste through distinct openings of the printing screen onto a given substrate. The layout of the printing screen can be designed in a flexible manner, for example, to accommodate multiple units of a single geometry and size or, alternatively, multiple units incorporating different geometries and sizes.

In this study, two screens with different layouts (disk and donut) were used (Fig. 1, Table S1). The resulting tablets therefore have a disk or a donut shape. The lateral tablet dimensions (diameter *D*, length *L*, width *W*) are specified by respective 2D layouts on the printing screen. However, the tablet height is dependent on the number of printed layers and their thickness (Table S2).

The feasibility of 3D printing a pharmaceutical DDS strongly depends on the rheological features of the ink. However, there is limited understanding on how to screen materials for rheological features and the limits that should be set as reference values for viscoelastic properties. Ideal printing inks should have a high viscosity, flowability under shear stress, and recovery of the viscosity to avoid further flow once the ink is deposited on the substrate or the precedent layer. Maintaining reproducibility and homogeneity of the ink formulation is a significant concern. Melt- or solution-based ink could phase separate during prolonged print periods, leading to inconsistencies in final tablets.

3DSP requires API loaded pastes to have specific rheological properties during the different printing phases to ensure successful printing. The printing process can be divided into 3 phases. In the first phase, the screen is flooded with the paste and the paste is distributed over the screen. The paste should fill the mesh openings. Filling is facilitated by shear thinning behavior of the paste. Once stress imposed by the squeegee ends, the paste is kept in the mesh openings by capillary forces. During the second phase, the printing phase, forces applied must thin the paste enough to extrude it through the mesh openings and transfer it onto the printing plate. As soon as the paste is on the printing plate, phase 3 begins. Here, the paste must regain its strength as quickly as possible to allow a stable form to build-up.

In order to investigate the physico-chemical characteristics of pastes and their suitability for 3DSP, rotational shear measurements were performed to provide insight on their shear rate dependent viscosity (Macosko, 1994). Both IR and ER pastes exhibited a decrease in viscosity as shear rates increased. This was already observable at shear rates of < 0.1 s^{-1} (Fig. 2**A**). This decrease is due to disentanglement and

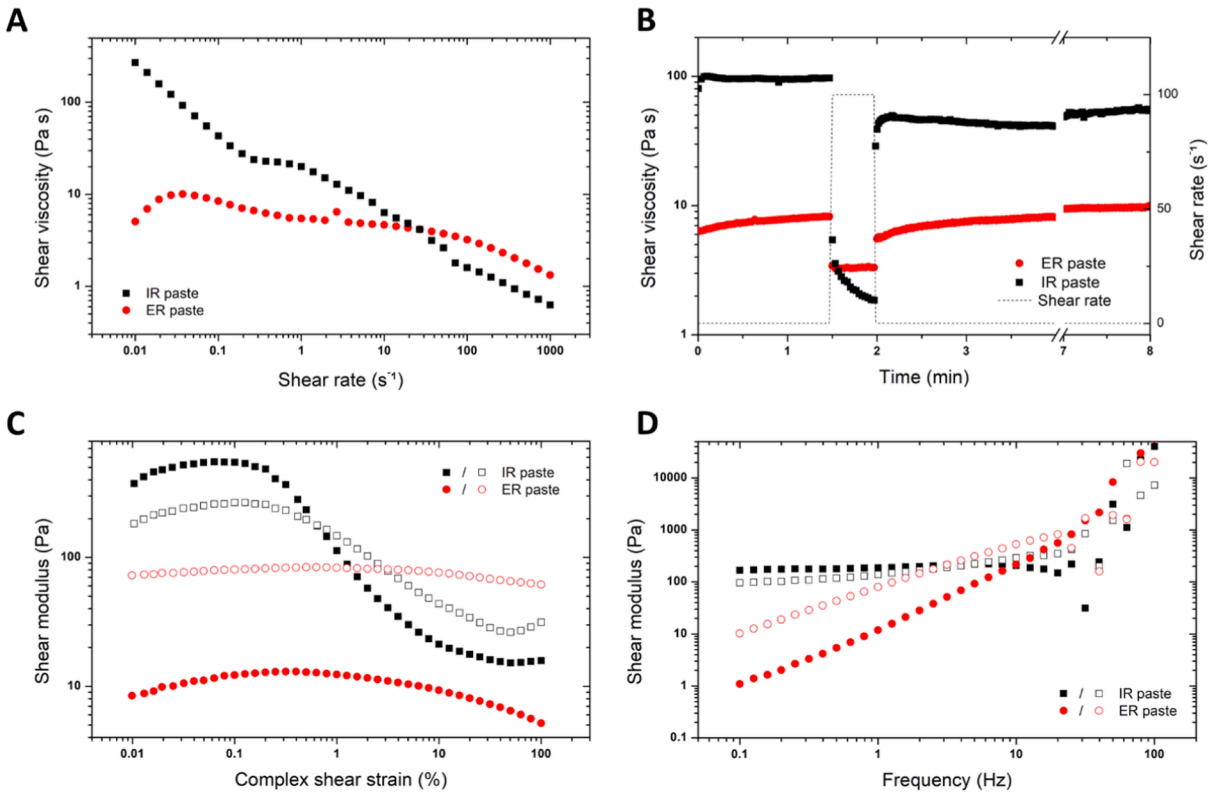

Fig. 2. Shear stress dependent viscosity **(A),** 3-step shear rate experiment **(B)**, amplitude sweep (frequency = 1 Hz) **(C)** and frequency sweep (strain = 0.05 %) **(D)** of IR (red) and ER (black) paste. Elastic and viscous component of the shear modulus are depicted as solid and hollow data points, respectively. (For interpretation of the references to color in this figure legend, the reader is referred to the web version of this article.)

orientation of the macromolecules such as hydroxypropyl cellulose (HPC) in the flow field (Masrat et al., 2016; Ramachandran et al., 1999). The difference in the shear viscosity curves can be explained by the different additional excipients used in paste formulation. In the IR paste, crosslinked N-vinyl-2-pyrrolidone is leading to a higher viscosity at low shear rates. This and the smaller molecular weight of the binder in comparison to the binder of the ER paste, leads to an increased shear thinning behavior. The large molecular weight of 140 kD of the ER binder and the microcrystalline cellulose (MCC) in the ER paste exhibit slightly different behavior, resulting from the organization of the MCC particles in the flow field (Ioelovich and Leykin, 2006). Increasing shear rates break up the contact between the MCC particles and thus a shear thinning can be observed at shear rates greater than 0.03 s^{-1}.

Since the shear rates to which pastes are exposed during the 3D screen printing process are remarkably higher (approx. around 10^3 s^{-1} for the flooding process and 10^5f s^{-1} or the printing process) than what can be measured with this setup, the process was simulated by a 3-step shear rate experiment (Fig. 2**B**). Here, a low shear rate of 0.1 s^{-1} is applied for 1.5 min. A higher shear rate of 100 s^{-1} is then applied for 0.5 min to resemble the flooding/printing process in 3DSP. The shear thinning properties of the pastes causes the viscosity to drop. The recovery of the pastes viscosity, and thereby their dimensional stability after removal of the shear force, can be observed when the shear rate is again lowered to 0.1 s^{-1}.

A strong difference was observed in the recovery of both IR and ER pastes. The ER paste exhibits thixotropic behavior, whereas the IR paste shows a fast recovery of its viscosity before increased shear. However, the initial viscosity at low shear rates is not reached even after 10 min. Nevertheless, the recovery of the initial viscosity of the ER paste is in the range of 101 s and thus still suitable for 3D printing as shown in printing tests. This incomplete but fast recovery might be due to irreversible changes in the microstructure of the paste. We attribute this to the presence of crosslinked N-vinyl-2-pyrrolidone (Polyplasdone Ultra 10) in the IR paste, which builds a strong elastic network due to crosslinking. By applying shear force, the structure might be altered to a large extent by breaking entanglements of polymer chains. However, the remaining crosslinks feature a strong driving force for regaining the shape and strength after the removal of the shear force.

To get further insight into the microstructure of the samples, oscillatory shear tests were conducted as previously described (Barnes, 2000; Rhon, 1995). By measuring the shear modulus in dependency of the applied strain (Fig. 2**C**), the viscous (loss modulus G'') and elastic (storage modulus G') nature of the sample can be evaluated. If G' > G'', the sample is of elastic nature. If G'' > G', the sample is viscously dominated. For the IR paste, it can be observed that up to a strain of 0.7 % the paste behaves "solid-like", meaning it is elastically dominated. At higher strains G' decreases and G'' increases and thus the sample is of viscous nature. This linear viscoelastic region (LVER) shows that the IR paste can be elastically deformed before the onset of structural breakdown at G' = G''. The LVER also gives insight into the stability of the paste. The elastic nature prevents sedimentation and could possibly extends shelf life. In contrast, the ER paste shows G'' > G' over the whole range of measured strains, representing its viscous nature. In frequency measurements of the IR paste (Fig. 2D), characteristics of a viscoelastic solid can be observed. The ER paste, in contrast, can be characterized as a viscoelastic liquid, consisting of weakly associated dispersion of particles. At low frequencies, "liquid-like" behavior is dominant. The frequency at G'' = G'' is equal $1/\tau$, with τ being the relaxation time, in this case $\tau = 0.083$ sec. This is the time scale on which stored elastic stresses are relaxed through rearrangement of the microstructure and converted to viscous stresses.

Overall, the variation in ingredients causes the two pastes to differ strongly in their rheological behavior. However, both are processable in 3DSP based on their shear thinning and structural recovery after stress removal.

3.2. Physical properties of printed tablets

Varying combinations of IR and ER pastes were used to create 10 tablet types (Fig. 3 example tablets; **Fig. S2**, schematic representation of pastes used). Manufacturing a batch for one component tablets needed 1 h to 1.5 h and a batch of two compartment tablets needed 2 to 2.5 h. The designed lateral tablet dimensions are summarized in **Table S1**. Physical parameters of printed disk-shaped tablets (Table 3) and donut-shaped tablets (Table 4) were measured. Compared with the lateral dimensions given from the screens, the measured ones were slightly smaller. Disk-shaped tablets differ on at maximum −4.5% from the screen layout and donut-shaped tablets showed a difference of −1.8%. The tablet height does not deviate greater than 7%. The decrease of the size of the tablets can be explained with the water evaporation during the printing process, which can be corrected by calculation the size reduction into the screen design. After production, the masses of the printed tablets were determined and showed an overall difference in the range of 2% and 7%. These data are comparable with other 3D screen printed tablets and provide evidence for the high precision of 3D screen printing (Goyanes et al., 2015b; Khaled et al., 2018; Korte and Quodbach, 2018; Robles Martinez et al., 2018).

These data show that tablets with a high degree of mass uniformity can be produced using the 3DSP technology presented. In terms of reproducibility of geometry and size as well as mass uniformity, 3DSP delivers results with the same high level of quality as other 3D printing techniques (Goyanes et al., 2015b; Khaled et al., 2018; Korte and Quodbach, 2018; Robles Martinez et al., 2018). Most importantly, results obtained comply with relevant regulatory requirements. Specifically, the specifications given by the Eur. Ph. for uncoated tablets allow deviations of up to ± 7.5% for average mass for tablets of 81–249 mg, and up to ± 10% for average mass for tablets ≤ 80 mg.

Table 5 summarizes the results of friability, hardness, and disintegration testing of all types of tablets. The friability of all tablet types is significantly lower than 1% and therefore conform with the Eur. Ph. The disk-shaped tablets revealed a higher hardness compared with the donut-shaped tablets. In addition, the tensile strength by Fell & Newton for disk-shaped tablets is presented (Fell and Newton, 1970). Here, values ranging from 0.91 and 1.38 MPa were obtained, which is within the range of tablets generated with other 3D printing methods (Chang et al., 2021; Shi et al., 2021). In general, tablets containing IR-paste have a higher hardness compared to tablets with the ER-paste. Overall, the breaking force appears to be high, and the printed tablets showed a high resistance to crushing considering the size of the tablets. However, donut-shaped tablets showed a significant lower hardness due to their design and break very easily by applying force in the lateral direction of the hole. Furthermore donut-shaped tablets demonstrated a faster disintegration time compared to disk-shaped tablets due to their higher surface-to-volume ratio. Interestingly, the difference is higher for IR-tablets compared with ER-tablets. Mixed tablets show also in their disintegration time the relationship of their ratios of IR- and ER-compartments. Therefore, more IR-compartment leads to a faster disintegration time. Overall, galenic testing of 3DSP tablets yielded results comparable with that of conventionally pressed tablets. Fig. 4 shows the disintegration time in dependency of the tablet geometry and the ratio of IR- and ER-compartment. It could be demonstrated that the donut-shaped tablet always has a faster disintegration compared to the disk-shaped tablet. Moreover, the greatest difference in the disintegration times could be seen between the tablet with 25% ER-compartment (IR/ER 1.5/0.5 tablet) and the tablet with 50% ER-compartment (IR/ER 1/1 tablet). This means the ER-compartment requires a critical thickness to influence the disintegration to longer times.

3.3. In vitro dissolution studies

It is already well established that the higher the surface-area-to-volume ratio (SA/V ratio) of a tablet, the faster API release will take

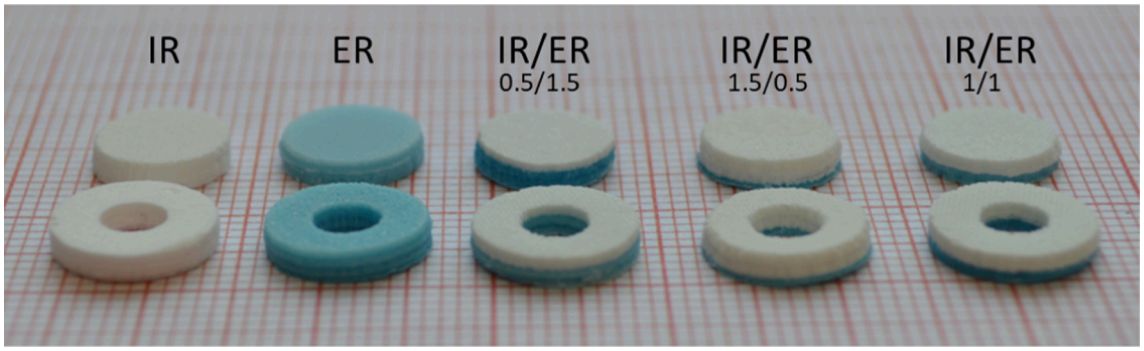

Fig. 3. Photographs of non-coated the 3D screen-printed tablets in disk- and donut-shape on millimeter paper. IR and ER pastes were made to produce ten different tablets. To improve visualization in combination tablets, the ER paste was colored blue. From left to right: IR, ER, IR/ER (0.5 mm:1.5 mm), IR/ER (1.5 mm:0.5 mm), and IR/ER (1 mm:1 mm). Non-coated tablet cores are shown. (For interpretation of the references to color in this figure legend, the reader is referred to the web version of this article.)

Table 3
Physical parameters of printed disk-shaped tablets: Diameter *D*, length *L*, height *H*, surface area *SA*, volume *V*, surface-area-to-volume-ratio *SA/V*, mass *m* and density ρ. Ten tablets of each geometry and size were weighted and measured with a digital caliper. *SA*, *V*, *SA/V* and ρ were calculated applying the relevant formulae. Measured values are given as average with standard deviation.

Shape (Size)	*D* [mm]	*H* [mm]	*SA* [mm^2]	*V* [mm^3]	*SA/V* [mm^{-1}]	*m* [mg]	ρ [mg mm^{-3}]
IR disk	8.75 ± 0.1	2.09 ± 0.02	177.7	125.7	1.41	118.03 ± 2.77	0.94
ER disk	8.92 ± 0.08	1.97 ± 0.08	180.2	123.1	1.46	130.12 ± 7.3	1.06
IR/ER 0.5/1.5	9.00 ± 0.08	1.99 ± 0.15	183.5	126.6	1.45	135.53 ± 3.51	1.07
IR/ER 1.5/0.5	9.04 ± 0.07	2.08 ± 0.09	187.4	133.5	1.40	126.14 ± 6.82	0.94
IR/ER 1/1	8.83 ± 0.08	2.03 ± 0.05	178.8	124.3	1.44	122.25 ± 2.61	0.98

Table 4
Physical parameters of printed donut-shaped tablets: Diameter *D* (outer, inner), length *L*, height *H*, surface area *SA*, volume *V*, surface-area-to-volume-ratio *SA/V*, mass *m* and density ρ. Ten tablets of each geometry and size were weighted and measured with a digital caliper. *V*, *SA/V* and ρ were calculated applying the relevant formulae. Measured values are given as average with standard deviation.

Shape (Size)	D_o [mm]	D_i [mm]	*H* [mm]	*SA* [mm^2]	*V* [mm^3]	SA/V [mm^{-1}]	*m* [mg]	ρ [mg mm^{-3}]
IR donut	10.09 ± 0.13	3.94 ± 0.13	2.14 ± 0.05	229.9	145.0	1.58	138.61 ± 6.91	0.96
ER donut	9.82 ± 0.13	4.21 ± 0.14	2.06 ± 0.06	214.4	127.3	1.68	134.13 ± 9.68	1.05
IR/ER 0.5/1.5	10.00 ± 0.1	4.02 ± 0.1	2.1 ± 0.05	224.2	138.3	1.62	142.35 ± 5.86	1.03
IR/ER 1.5/0.5	9.94 ± 0.07	4.21 ± 0.17	2.24 ± 0.04	226.9	142.6	1.59	118.44 ± 1.88	0.83
IR/ER 1/1	10.18 ± 0.07	3.89 ± 0.09	2.1 ± 0.05	231.8	146.0	1.59	143.22 ± 4.86	0.81

Table 5
Results from friability, hardness, and disintegration testing of disk- and donut-shaped tablets.

	Disk				Donut		
Tablets	Friability [%]	Hardness [N]	Tensile strength [MPa]	Disintegration [mm:ss]	Friability [%]	Hardness [N]	Disintegration [mm:ss]
IR	0.237	39.0 ± 3.0	1.36	4:41 ± 0:45	0.160	16.3 ± 0.7	2:37 ± 0:26
ER	0.002	25.1 ± 1.8	0.91	102:51 ± 9:15	0.016	–*	81:32 ± 8:02
IR/ER 0.5/1.5	0.009	29.9 ± 1.7	1.06	85:17 ± 19:34	0.124	–*	50:25 ± 8:22
IR/ER 1.5/0.5	0.099	34.1 ± 1.9	1.15	17:57 ± 1:40	0.072	–*	13:00 ± 1:54
IR/ER 1/1	0.066	37.8 ± 2.0	1.34	64:01 ± 5:32	0.053	–*	38.42 ± 6.46

* Donut-shaped tablets break in the middle and get further pressed together, afterwards hardness is measured.

place (Brooke and Washkuhn, 1977; Ford et al., 1987; Reynolds et al., 2002). Our group has already shown a correlation of the rate of Paracetamol release to the SA/V ratios for different sizes and designed geometries (disk, donut, cuboid, oval and grid) of tablets using a delayed release paste (Moldenhauer et al., 2021). These data are on par with drug release profiles obtained from other 3DP technologies such as binder jetting, fused deposition modelling and semi-solid extrusion (Goyanes et al., 2015c, 2015b; Khaled et al., 2018, 2014).

To see if this paradigm was upheld for DDS made of pastes with different API release profiles and composite DDS exhibiting 2-compartments built with each of the different pastes, respective DDS were subjected to dissolution testing. Overall, API release from 3DSP tablets for the tested tablet geometries and pastes paralleled the SA/V (disk-shaped tablets: ~ 1.4 mm^{-1} and donut-shaped tablets: ~ 1.6 mm^{-1}) ratios, which was more evident for ER paste formulation (Fig. 5). Moreover, IR tablets (both donut and disk) showed faster API-release compared to ER tablets of the same geometry (Fig. 5). More importantly, API release could be controlled by fabricating 2-compartment DDS by varying the size of the ER- and IR compartments. IR tablets (donut) took 15 min to reach over 80% API release, whereas the ER tablets (donut) needed 95 min for over 80% API release. The API release of the 2-compartment tablets was between these two extremes and depended on the ER/IR ratio. IR/ER 1.5/0.5 donut required 25 min for over 80% API release, whereas IR/ER 0.5/1.5 tablets 80 min for over 80% API release. IR/ER

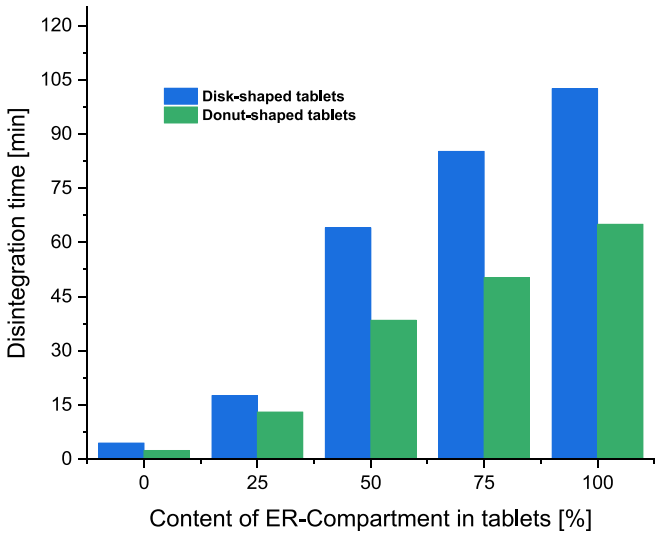

Fig. 4. Diagram demonstrating the disintegration time and their ratios depending on the different tablets and their IR/ER ratio.

1/1 tablets needed 45 min for over 80% API release. Similar data were obtained for the disk geometry. In this context, it was important to note that the 2 compartments did not separate from each other during dissolution testing. API release of the different DDS was also analyzed based on percentage of API release per time interval. Tablets made of the ER paste showed a lower maximum, but a longer release compared to the IR paste tablets. Composite tablets containing both IR- and ER compartments demonstrated a broadening of the peaks and a lower maximum as a function of the tablets ER proportion (Fig. 6).

4. Conclusions

The current study describes the fabrication of a 2-compartment DDS using 3DSP. In the example presented, the two compartments differ by their API release profiles. The IR formulation enables 80% of Paracetamol release (from the donut geometry) to occur within 15 min, whereas the ER formulation is characterized by 80% drug release by 95 min. By varying the polymer, it will be possible to design and generate ER pastes characterized by more extended drug release. By integrating IR and ER formulations into a DDS and varying the proportions of the resulting ER- and IR compartments, the drug release profiles can be further tailored to a medical need based on the drug and the indication.

A key feature of 3DP technologies is the ability to readily vary ER/IR

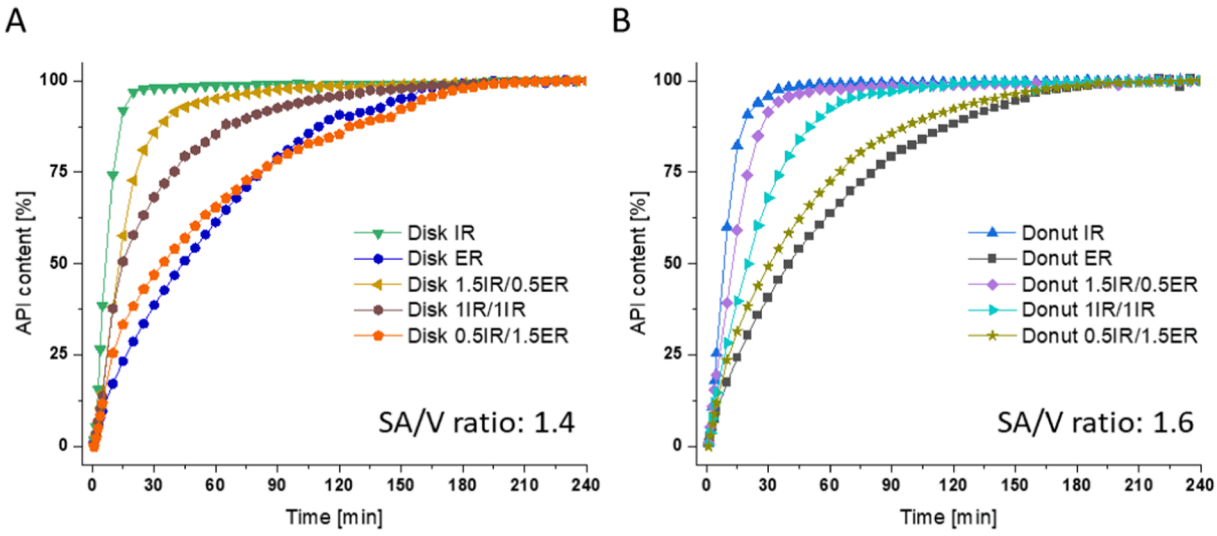

Fig. 5. Dissolution profile of 3D screen-printed tablet comparing (A) disk- and (B) donut-shaped tablets.

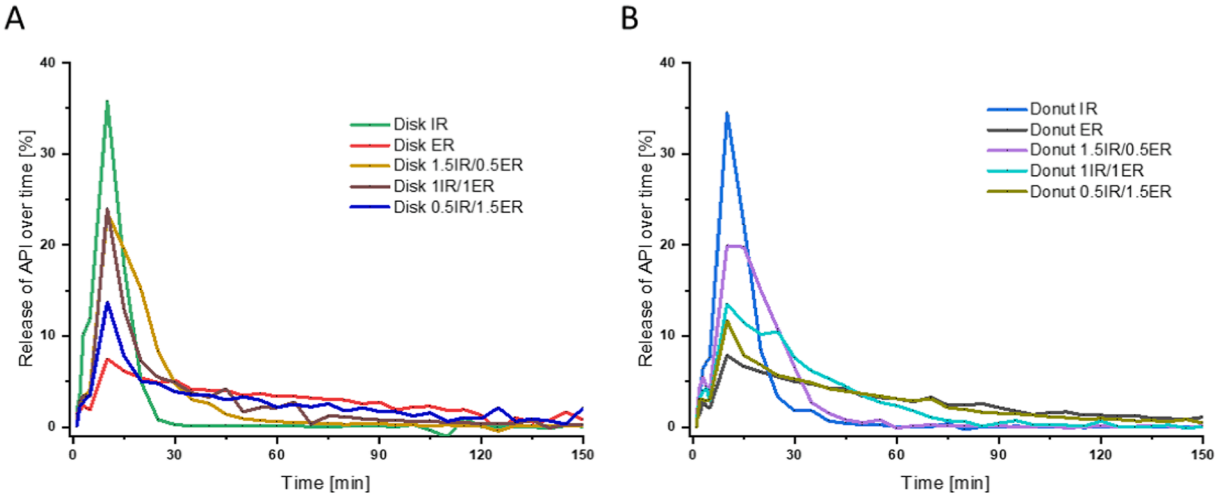

Fig. 6. Dissolution profile of (A) disk- and (B) donut-shaped tablets plotted in behave of their release of paracetamol every 5 min.

proportions within the composite DDS by adapting the number and/or thickness of the layers of each formulation. Multiple studies have previously demonstrated combinations of IR and ER compartments going back over 20 years (Rowe et al., 2000). Data presented demonstrate the feasibility of producing composite DDS with tailored drug release profiles using 3DSP technology. This is important to ensure that the technology is competitive with existing 3DP approaches.

The difference in the release profiles of the 2-compartment tablets is primarily due to the type and amount of polymer used in the formulations. Various other polymers are available and can be used with the 3DSP technology. These include among others Benecel™ (HPMC), Natrosol™ (HEC) and new Klucel Xtend™ (HPC). Varying the polymer may allow for an even broader spectrum of drug release profiles.

The study highlights the strength and potential of 3DSP. The ability to regulate the release of a pain killer as described here would facilitate pain management, as one could achieve quick and prolonged activity with a single tablet. Additional work is needed to create tablets with even longer release profiles. Preliminary results have already been achieved for tablets using ER pastes with release profiles of 5 to 6 h (data not shown). Further work is also needed to test the incorporation of different APIs in the 2 different compartments of the tablet providing further functionality to the DDS. For example, the strategy outlined here could be used to facilitate the sequential release of Carbidopa and Levodopa to enhance the efficacy of the golden standard drug for the management of Parkinson's disease.

CRediT authorship contribution statement

Marcel Enke: Conceptualization, Methodology, Formal analysis, Writing – original draft. **Nicolle Schwarz:** Investigation. **Franka Gruschwitz:** Investigation, Methodology. **Daniela Winkler:** Investigation. **Felix Hanf:** Investigation. **Lisa Jescheck:** Investigation. **Stefan Seyferth:** Investigation, Writing – review & editing. **Dagmar Fischer:** Writing – review & editing. **Achim Schneeberger:** Conceptualization, Writing – review & editing, Supervision, Validation.

Declaration of Competing Interest

The authors declare the following financial interests/personal relationships which may be considered as potential competing interests: Achim Schneeberger reports a relationship with Laxxon Medical GmbH that includes: employment. Marcel Enke reports a relationship with Laxxon Medical GmbH that includes: employment. Nicolle Schwarz reports a relationship with Laxxon Medical GmbH that includes: employment. Franka Gruschwitz reports a relationship with Laxxon Medical GmbH that includes: employment. Daniela Winkler reports a relationship with Laxxon Medical GmbH that includes: employment. Felix Hanf reports a relationship with Laxxon Medical GmbH that includes: employment. Lisa Jescheck reports a relationship with Laxxon Medical GmbH that includes: employment.

Data availability

Data will be made available on request.

Appendix A. Supplementary material

Supplementary data to this article can be found online at https://doi.org/10.1016/j.ijpharm.2023.123101.

References

Alhnan, M.A., Okwuosa, T.C., Sadia, M., Wan, K.-W., Ahmed, W., Arafat, B., 2016. Emergence of 3D Printed Dosage Forms: Opportunities and Challenges. Pharm. Res. 33, 1817–1832. https://doi.org/10.1007/s11095-016-1933-1.

Awad, A., Gaisford, S., Basit, A.W., 2018. Fused Deposition Modelling: Advances in Engineering and Medicine. In: Basit, A.W., Gaisford, S. (Eds.), 3D Printing of Pharmaceuticals, AAPS Advances in the Pharmaceutical Sciences Series. Springer International Publishing, Cham, pp. 107–132. https://doi.org/10.1007/978-3-319-90755-0_6.

Awad, A., Fina, F., Trenfield, S., Patel, P., Goyanes, A., Gaisford, S., Basit, A., 2019. 3D Printed Pellets (Miniprintlets): A Novel, Multi-Drug, Controlled Release Platform Technology. Pharmaceutics 11, 148. https://doi.org/10.3390/pharmaceutics11040148.

Awad, A., Fina, F., Goyanes, A., Gaisford, S., Basit, A.W., 2020. 3D printing: Principles and pharmaceutical applications of selective laser sintering. Int. J. Pharm. 586, 119594 https://doi.org/10.1016/j.ijpharm.2020.119594.

Barnes, H.A., 2000. Handbook of Elementary Rheology, Institute of non-newtonian Fluid mechanics. University of Wales.

Beg, S., Almalki, W.H., Malik, A., Farhan, M., Aatif, M., Rahman, Z., Alruwaili, N.K., Alrobaian, M., Tarique, M., Rahman, M., 2020. 3D printing for drug delivery and biomedical applications. Drug Discov. Today 25, 1668–1681. https://doi.org/10.1016/j.drudis.2020.07.007.

Brooke, D., Washkuhn, R.J., 1977. Zero-Order Drug Delivery System: Theory and Preliminary Testing. J. Pharm. Sci. 66, 159–162. https://doi.org/10.1002/jps.2600660206.

Cader, H.K., Rance, G.A., Alexander, M.R., Gonçalves, A.D., Roberts, C.J., Tuck, C.J., Wildman, R.D., 2019. Water-based 3D inkjet printing of an oral pharmaceutical dosage form. Int. J. Pharm. 564, 359–368. https://doi.org/10.1016/j.ijpharm.2019.04.026.

Chang, S.-Y., Jin, J., Yan, J., Dong, X., Chaudhuri, B., Nagapudi, K., Ma, A.W.K., 2021. Development of a pilot-scale HuskyJet binder jet 3D printer for additive manufacturing of pharmaceutical tablets. Int. J. Pharm. 605, 120791 https://doi.org/10.1016/j.ijpharm.2021.120791.

El Aita, I., Ponsar, H., Quodbach, J., 2019. A Critical Review on 3D-printed Dosage Forms. CPD 24, 4957–4978. https://doi.org/10.2174/1381612825666181206124206.

Elbadawi, M., McCoubrey, L.E., Gavins, F.K.H., Ong, J.J., Goyanes, A., Gaisford, S., Basit, A.W., 2021. Disrupting 3D printing of medicines with machine learning. Trends Pharmacol. Sci. 42, 745–757. https://doi.org/10.1016/j.tips.2021.06.002.

Enke, M., Kühne, K., Seyferth, S., Fischer, D., Schneeberger, A., 2022. 3D Screen Printing Enables Application of Integrated QR Codes on Pharmaceutical Dosage Forms in Mass Production – A Game Changer. BJSTR 41. https://doi.org/10.26717/BJSTR.2022.41.006630.

Fell, J.T., Newton, J.M., 1970. Determination of Tablet Strength by the Diametral-Compression Test. J. Pharm. Sci. 59, 688–691. https://doi.org/10.1002/jps.2600590523.

Firth, J., Basit, A.W., Gaisford, S., 2018. The Role of Semi-Solid Extrusion Printing in Clinical Practice. In: Basit, A.W., Gaisford, S. (Eds.), 3D Printing of Pharmaceuticals, AAPS Advances in the Pharmaceutical Sciences Series. Springer International Publishing, Cham, pp. 133–151. https://doi.org/10.1007/978-3-319-90755-0_7.

Ford, J.L., Rubinstein, M.H., McCaul, F., Hogan, J.E., Edgar, P.J., 1987. Importance of drug type, tablet shape and added diluents on drug release kinetics from hydroxypropylmethylcellulose matrix tablets. Int. J. Pharm. 40, 223–234. https://doi.org/10.1016/0378-5173(87)90172-4.

Goyanes, A., Buanz, A.B.M., Hatton, G.B., Gaisford, S., Basit, A.W., 2015a. 3D printing of modified-release aminosalicylate (4-ASA and 5-ASA) tablets. Eur. J. Pharm. Biopharm. 89, 157–162. https://doi.org/10.1016/j.ejpb.2014.12.003.

Goyanes, A., Robles Martinez, P., Buanz, A., Basit, A.W., Gaisford, S., 2015b. Effect of geometry on drug release from 3D printed tablets. Int. J. Pharm. 494, 657–663. https://doi.org/10.1016/j.ijpharm.2015.04.069.

Goyanes, A., Wang, J., Buanz, A., Martínez-Pacheco, R., Telford, R., Gaisford, S., Basit, A.W., 2015c. 3D Printing of Medicines: Engineering Novel Oral Devices with Unique Design and Drug Release Characteristics. Mol. Pharm. 12, 4077–4084. https://doi.org/10.1021/acs.molpharmaceut.5b00510.

Hsiao, W.-K., Lorber, B., Reitsamer, H., Khinast, J., 2018. 3D printing of oral drugs: a new reality or hype? Expert Opin. Drug Deliv. 15, 1–4. https://doi.org/10.1080/17425247.2017.1371698.

Infanger, S., Haemmerli, A., Iliev, S., Baier, A., Stoyanov, E., Quodbach, J., 2019. Powder bed 3D-printing of highly loaded drug delivery devices with hydroxypropyl cellulose as solid binder. Int. J. Pharm. 555, 198–206. https://doi.org/10.1016/j.ijpharm.2018.11.048.

Ioelovich, M., Leykin, A., 2006. Structural characteristics and rheological properties of microcrystalline cellulose. Cellulose Chem. Technol. 40 (9–10), 699–703.

Jamróz, W., Szafraniec, J., Kurek, M., Jachowicz, R., 2018. 3D Printing in Pharmaceutical and Medical Applications – Recent Achievements and Challenges. Pharm. Res. 35, 176. https://doi.org/10.1007/s11095-018-2454-x.

Jose, P.A., Gv, P.C., 2018. 3D printing of pharmaceuticals – A potential technology in developing personalized medicine. Asian J. Pharm. Res. Dev. 6, 46–54. https://doi.org/10.22270/ajprd.v6i3.375.

Jurisch, M., Studnitzky, T., Andersen, O., Kieback, B., 2015. 3D screen printing for the fabrication of small intricate Ti-6Al-4V parts. Powder Metall. 58, 339–343. https://doi.org/10.1179/0032589915Z.000000000255.

Khairuzzaman, A., 2018. Regulatory Perspectives on 3D Printing in Pharmaceuticals. In: Basit, A.W., Gaisford, S. (Eds.), 3D Printing of Pharmaceuticals, AAPS Advances in the Pharmaceutical Sciences Series. Springer International Publishing, Cham, pp. 215–236. https://doi.org/10.1007/978-3-319-90755-0_11.

Khaled, S.A., Burley, J.C., Alexander, M.R., Roberts, C.J., 2014. Desktop 3D printing of controlled release pharmaceutical bilayer tablets. Int. J. Pharm. 461, 105–111. https://doi.org/10.1016/j.ijpharm.2013.11.021.

Khaled, S.A., Alexander, M.R., Irvine, D.J., Wildman, R.D., Wallace, M.J., Sharpe, S., Yoo, J., Roberts, C.J., 2018. Extrusion 3D Printing of Paracetamol Tablets from a Single Formulation with Tunable Release Profiles Through Control of Tablet

Geometry. AAPS PharmSciTech 19, 3403–3413. https://doi.org/10.1208/s12249-018-1107-z.
Kipphan, H. (Ed.), 2001. Handbook of Print Media. Springer, Berlin Heidelberg, Berlin, Heidelberg. https://doi.org/10.1007/978-3-540-29900-4.
Korte, C., Quodbach, J., 2018. 3D-Printed Network Structures as Controlled-Release Drug Delivery Systems: Dose Adjustment, API Release Analysis and Prediction. AAPS PharmSciTech 19, 3333–3342. https://doi.org/10.1208/s12249-018-1017-0.
Kyobula, M., Adedeji, A., Alexander, M.R., Saleh, E., Wildman, R., Ashcroft, I., Gellert, P. R., Roberts, C.J., 2017. 3D inkjet printing of tablets exploiting bespoke complex geometries for controlled and tuneable drug release. J. Control. Release 261, 207–215. https://doi.org/10.1016/j.jconrel.2017.06.025.
Macosko, C.W., 1994. Rheology: principles, measurements, and applications, Advances in interfacial engineering series. VCH, New York, NY.
Masrat, R., Maswal, M., Chat, O.A., Rather, G.M., Dar, A.A., 2016. A rheological investigation of sol–gel transition of hydroxypropyl cellulose with nonionic surfactant sorbitan monopalmitate: Modulation of gel strength by UV irradiation. Colloids Surf. A Physicochem. Eng. Asp 489, 113–121. https://doi.org/10.1016/j.colsurfa.2015.10.012.
Melnyk, L.A., Oyewumi, M.O., 2021. Integration of 3D printing technology in pharmaceutical compounding: Progress, prospects, and challenges. Ann. 3D Printed Med. 4, 100035 https://doi.org/10.1016/j.stlm.2021.100035.
Mirza, Mohd.A., Iqbal, Z., 2019. 3D Printing in Pharmaceuticals: Regulatory Perspective. CPD 24, 5081–5083. https://doi.org/10.2174/1381612825666181130163027.
Moldenhauer, D., Nguyen, D.C.Y., Jescheck, L., Hack, F., Fischer, D., Schneeberger, A., 2021. 3D screen printing – An innovative technology for large-scale manufacturing of pharmaceutical dosage forms. Int. J. Pharm. 592, 120096 https://doi.org/10.1016/j.ijpharm.2020.120096.
Norman, J., Madurawe, R.D., Moore, C.M.V., Khan, M.A., Khairuzzaman, A., 2017. A new chapter in pharmaceutical manufacturing: 3D-printed drug products. Adv. Drug Deliv. Rev. 108, 39–50. https://doi.org/10.1016/j.addr.2016.03.001.
Peck, R.W., 2021. Precision Dosing: An Industry Perspective. Clin. Pharma Therapeut. 109, 47–50. https://doi.org/10.1002/cpt.2064.
Pietrzak, K., Isreb, A., Alhnan, M.A., 2015. A flexible-dose dispenser for immediate and extended release 3D printed tablets. Eur. J. Pharm. Biopharm. 96, 380–387. https://doi.org/10.1016/j.ejpb.2015.07.027.
Ramachandran, S., Chen, S., Etzler, F., 1999. Rheological Characterization of Hydroxypropylcellulose Gels. Drug Dev. Ind. Pharm. 25, 153–161. https://doi.org/10.1081/DDC-100102155.
Research and Markets, 2022. Oral Drug Delivery Market - Forecasts from 2022 to 2027 [WWW Document]. URL https://www.researchandmarkets.com/reports/5602457/oral-drug-delivery-market-forecasts-from-2022 (accessed 9.1.22).
Reynolds, T.D., Mitchell, S.A., Balwinski, K.M., 2002. Investigation of the Effect of Tablet Surface Area/Volume on Drug Release from Hydroxypropylmethylcellulose Controlled-Release Matrix Tablets. Drug Dev. Ind. Pharm. 28, 457–466. https://doi.org/10.1081/DDC-120003007.
Rhon, C.L., 1995. Analytical Polymer Rheology: Structure-Processing-Property Relationships. Hanser Gardner Publisher Inc., Cincinnati.
Robles Martinez, P., Basit, A.W., Gaisford, S., 2018. The History, Developments and Opportunities of Stereolithography. In: Basit, A.W., Gaisford, S. (Eds.), 3D Printing of Pharmaceuticals, AAPS Advances in the Pharmaceutical Sciences Series. Springer International Publishing, Cham, pp. 55–79. https://doi.org/10.1007/978-3-319-90755-0_4.
Rowe, C.W., Katstra, W.E., Palazzolo, R.D., Giritlioglu, B., Teung, P., Cima, M.J., 2000. Multimechanism oral dosage forms fabricated by three dimensional printing™. J. Control. Release 66, 11–17. https://doi.org/10.1016/S0168-3659(99)00224-2.
Schröder, T., 2018. Rheologie der Kunststoffe: Theorie und Praxis. Hanser, München.
Seoane-Viaño, I., Trenfield, S.J., Basit, A.W., Goyanes, A., 2021. Translating 3D printed pharmaceuticals: From hype to real-world clinical applications. Adv. Drug Deliv. Rev. 174, 553–575. https://doi.org/10.1016/j.addr.2021.05.003.
Shi, K., Salvage, J.P., Maniruzzaman, M., Nokhodchi, A., 2021. Role of release modifiers to modulate drug release from fused deposition modelling (FDM) 3D printed tablets. Int. J. Pharm. 597, 120315 https://doi.org/10.1016/j.ijpharm.2021.120315.
Tracy, T., Wu, L., Liu, X., Cheng, S., Li, X., 2023. 3D printing: Innovative solutions for patients and pharmaceutical industry. Int. J. Pharm. 631, 122480 https://doi.org/10.1016/j.ijpharm.2022.122480.
Trenfield, S.J., Madla, C.M., Basit, A.W., Gaisford, S., 2018. Binder Jet Printing in Pharmaceutical Manufacturing. In: Basit, A.W., Gaisford, S. (Eds.), 3D Printing of Pharmaceuticals, AAPS Advances in the Pharmaceutical Sciences Series. Springer International Publishing, Cham, pp. 41–54. https://doi.org/10.1007/978-3-319-90755-0_3.
Trenfield, S.J., Awad, A., Madla, C.M., Hatton, G.B., Firth, J., Goyanes, A., Gaisford, S., Basit, A.W., 2019. Shaping the future: recent advances of 3D printing in drug delivery and healthcare. Expert Opin. Drug Deliv. 16, 1081–1094. https://doi.org/10.1080/17425247.2019.1660318.
Triastek, Inc., 2022. Triastek Receives FDA IND Clearance for 3D Printed Medicine for the Treatment of Ulcerative Colitis. prnewswire CISION.
Varghese, R., Sood, P., Salvi, S., Karsiya, J., Kumar, D., 2022. 3D printing in the pharmaceutical sector: Advances and evidences. Sensors International 3, 100177. https://doi.org/10.1016/j.sintl.2022.100177.
Wang, C.-C., Tejwani (Motwani), M.R., Roach, W.J., Kay, J.L., Yoo, J., Surprenant, H.L., Monkhouse, D.C., Pryor, T.J., 2006. Development of Near Zero-Order Release Dosage Forms Using Three-Dimensional Printing (3-DP™) Technology. Drug Develop. Ind. Pharm. 32, 367–376. https://doi.org/10.1080/03639040500519300.
West, T.G., Bradbury, T.J., 2018. 3D Printing: A Case of ZipDose® Technology - World's First 3D Printing Platform to Obtain FDA Approval for a Pharmaceutical Product. In: Maniruzzaman, M. (Ed.), 3D and 4D Printing in Biomedical Applications. Wiley-VCH Verlag GmbH & Co. KGaA, Weinheim, Germany, pp. 53–79. https://doi.org/10.1002/9783527813704.ch3.
Yu, D.G., Yang, X.L., Huang, W.D., Liu, J., Wang, Y.G., Xu, H., 2007. Tablets With Material Gradients Fabricated by Three-Dimensional Printing. J. Pharm. Sci. 96, 2446–2456. https://doi.org/10.1002/jps.20864.
Zhu, X., Li, H., Huang, L., Zhang, M., Fan, W., Cui, L., 2020. 3D printing promotes the development of drugs. Biomed. Pharmacother. 131, 110644 https://doi.org/10.1016/j.biopha.2020.110644.